

Laplace's equation for a point source near a sphere: improved internal solution using spheroidal harmonics

Matt R. A. Majić, Baptiste Auguié, and Eric C. Le Ru*

*The MacDiarmid Institute for Advanced Materials and Nanotechnology, School of Chemical and Physical Sciences,
Victoria University of Wellington, PO Box 600, Wellington 6140, New Zealand*

(Dated: December 14, 2024)

As shown recently [Phys. Rev. E 95, 033307 (2017)], spheroidal harmonics expansions are well suited for the external solution of Laplace's equation for a point source outside a spherical object. Their intrinsic singularity matches the line singularity of the analytic continuation of the solution and the series solution converges much faster than the standard spherical harmonic solution. Here we extend this approach to internal potentials using the Kelvin transformation, ie. radial inversion, of the spheroidal coordinate system. This transform converts the standard series solution involving regular solid spherical harmonics into a series of irregular spherical harmonics. We then substitute the expansion of irregular spherical harmonics in terms of transformed irregular spheroidal harmonics into the potential. The spheroidal harmonic solution fits the image line singularity of the solution exactly and converges much faster. We also discuss why a solution in terms of regular spheroidal harmonics cannot work, even though these functions are finite everywhere in the sphere. We also present the analogous solution for an internal point source, and two new relationships between the spherical and spheroidal harmonics.

I. INTRODUCTION

We have recently demonstrated that spheroidal harmonics can be used to improve the solution of Laplace's equation for a point source outside a sphere close to its surface [1]. Specifically, we found the solution outside the sphere expanded as a simple spheroidal harmonic series, which converges much faster than the standard spherical harmonic series. This is intriguing as the spherical coordinate system initially appeared as more natural. Here we consider the solution inside the sphere for the same problem. For the sake of argument, we will focus on the electrostatics problem of a point charge near a dielectric sphere, but the conclusions can be easily extended to any multipolar point source and to other physical systems governed by Laplace's equation.

The method we previously used to express the external potential in terms of spheroidal harmonics is to substitute the expansion of irregular spherical harmonics in terms of irregular spheroidal harmonics into the standard series solution and rearrange the order of summation [1]. For internal potentials, the standard solution is a series of regular solid spherical harmonics, so it would seem natural to substitute the expansion of regular solid spherical harmonics in terms of regular solid spheroidal harmonics. To this end, we present and prove (see Appendix) two relationships between the spherical and offset spheroidal harmonics, similar to the ones presented in [1]. However, as discussed in detail in section III, this approach fails to produce a suitable solution. Instead, as presented in Sec. II, the spherical solution can be manipulated by radial inversion ($r \rightarrow 1/r$), as first discussed by Kelvin in 1845 [2] and often known as the Kelvin transformation. This

transform is a conformal mapping often used to transform the geometry of a complex problem into a simpler geometry in which the solution is known [3, 4]. We apply the transform to turn the sphere inside out, so that the problem becomes equivalent to finding the external potential in the transformed frame. We can then follow the same method as in [1] to obtain the solution as a series of transformed irregular spheroidal harmonics. The new series solution converges much faster than the standard spherical harmonics solution. We also show in Sec. IV that the case of a point charge inside the sphere can be treated using a similar approach.

This work further highlights the usefulness of spheroidal harmonics in non-spheroidal geometry. As in [1], these results can be understood in terms of the location of the singularity of the solution. We show that the singularities of the radially inverted spheroidal harmonics lie exactly on the image line charge derived in [5, 6]. This approach also leads us to introduce an uncommon type of coordinates: radially-inverted offset prolate spheroidal coordinates, a partially separable coordinate system of the Laplacian.

II. POINT CHARGE OUTSIDE THE SPHERE

We consider the same problem as in Ref. [1], shown schematically in Fig. 1. For convenience, we write the potential as $V = \vec{V} \cdot \vec{q}/(4\pi\epsilon_0\epsilon_1 a)$ and work with the dimensionless \vec{V} . The potential outside the sphere is $\vec{V}_{\text{out}} = \vec{V}_q + \vec{V}_r$, where \vec{V}_q is the potential of the point charge and \vec{V}_r the reflected potential. \vec{V}_{in} is the potential inside the sphere. The standard solution in spherical

* eric.leru@vuw.ac.nz

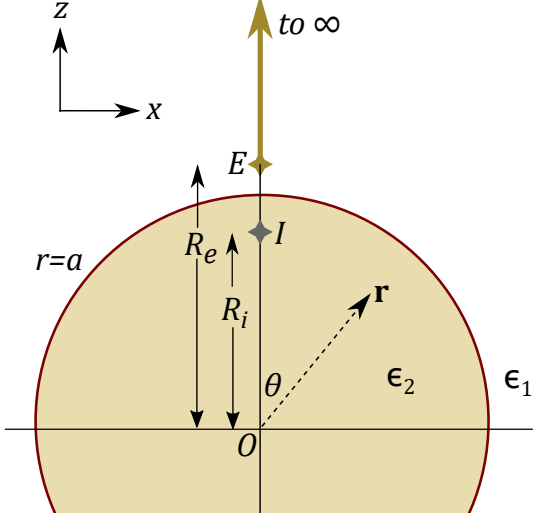


FIG. 1. Schematic of the problem considered in this work. A point charge q is located at point E (external) outside a dielectric sphere of radius a , on the z -axis a distance R_e from the origin. Point I (internal) located at $z = R_i = a^2/R_e$ is the location of the image charge in the standard solution for the outside potential. The relative permittivity of the sphere with respect to the surroundings is $\epsilon = \epsilon_2/\epsilon_1$. The line from E to infinity is the location of the image line charge used in the solution of the internal potential within the method of images [5]. The external solution was studied in Ref. [1] and we focus on the internal solution in Secs. II and III. Sec. IV considers the case where the point charge q is located inside the sphere at point I.

coordinates (r, θ, ϕ) is [5, 7]:

$$\bar{V}_q = \frac{a}{|\mathbf{r} - R_e \hat{z}|} = \frac{a}{R_e} \sum_{n=0}^{\infty} \left(\frac{r}{R_e}\right)^n P_n(\cos \theta) \quad (r < R_e), \quad (1)$$

$$\bar{V}_r = -\sum_{n=0}^{\infty} \beta_n \left(\frac{R_i}{r}\right)^{n+1} P_n(\cos \theta) \quad (r \geq a), \quad (2)$$

$$\bar{V}_{\text{in}} = \frac{a}{R_e} \sum_{n=0}^{\infty} \frac{2n+1}{n(\epsilon+1)+1} \left(\frac{r}{R_e}\right)^n P_n(\cos \theta) \quad (r \leq a), \quad (3)$$

where $R_i = a^2/R_e$, P_n are the Legendre polynomials, and

$$\beta_n = \frac{n(\epsilon-1)}{n(\epsilon+1)+1}, \quad \text{with } \beta_{\infty} = \frac{\epsilon-1}{\epsilon+1}. \quad (4)$$

These series are slowly convergent close to the sphere surface ($r \rightarrow a$), especially for a source close to the surface ($|R_e - a| \ll a$).

A. External potential

In Ref. [1], a much more rapidly convergent series in terms of spheroidal harmonics was derived for the reflected potential \bar{V}_r using spheroidal coordinates $(\bar{\xi}, \bar{\eta}, \phi)$ with foci located at points O and I. This was achieved by expanding the irregular spherical harmonics in Eq. 2 in terms of irregular spheroidal harmonics $Q_n(\bar{\xi})P_n(\bar{\eta})$ (see Eq. A3), where Q_n denotes the Legendre functions of the second kind. The resulting expression for the reflected potential is

$$\bar{V}_r = -\beta_{\infty} \frac{R_i}{r'} + 2\beta_{\infty} \sum_{n=0}^{\infty} (2n+1)c_n Q_n(\bar{\xi})P_n(\bar{\eta}). \quad (5)$$

The first term on the right corresponds to an image charge, with $r' = \sqrt{r^2 - 2R_i r \cos \theta + R_i^2}$.

The coefficients in this solution can be expressed as a sum or a product:

$$\begin{aligned} c_n &= \mu \sum_{k=0}^n \frac{(n+k)!}{(n-k)!k!2} \frac{(-)^{n+k}}{k+\mu} \\ &= \prod_{k=0}^n \frac{\mu-k}{\mu+k}, \quad \mu = \frac{1}{\epsilon+1}. \end{aligned} \quad (6)$$

B. Internal potential

We now apply the same approach to the internal potential. Following [1], we first separate the dominant term:

$$\frac{2n+1}{n(\epsilon+1)+1} = \frac{2}{\epsilon+1} + \frac{\beta_{\infty}}{n(\epsilon+1)+1}, \quad (7)$$

and recognize the sum over the constant term as \bar{V}_q :

$$\bar{V}_{\text{in}} = \frac{2\bar{V}_q}{\epsilon+1} + \frac{a}{R_e} \sum_{n=0}^{\infty} \frac{\beta_{\infty}}{n(\epsilon+1)+1} \left(\frac{r}{R_e}\right)^n P_n(\cos \theta). \quad (8)$$

From here the natural approach would be to expand the regular spherical harmonics in terms of regular spheroidal harmonics. However, for reasons discussed in the next section, this approach does not work.

Instead we use the Kelvin transformation to transform the expression into one that is very similar to that of the reflected potential. The Kelvin transformation is an inversion of the radial coordinate and is defined in [3, 4]:

$$\check{r} = \frac{a^2}{r}, \quad \check{R}_e = \frac{a^2}{R_e} = R_i, \quad (9)$$

and θ, ϕ are unchanged. With the transformed coordinates, Eq. 8 becomes (for $\check{r} \geq a$)

$$\bar{V}_{\text{in}} = \frac{2\bar{V}_q}{\epsilon+1} + \frac{a}{r} \sum_{n=0}^{\infty} \frac{\beta_{\infty}}{n(\epsilon+1)+1} \left(\frac{\check{R}_e}{\check{r}}\right)^{n+1} P_n(\cos \theta) \quad (10)$$

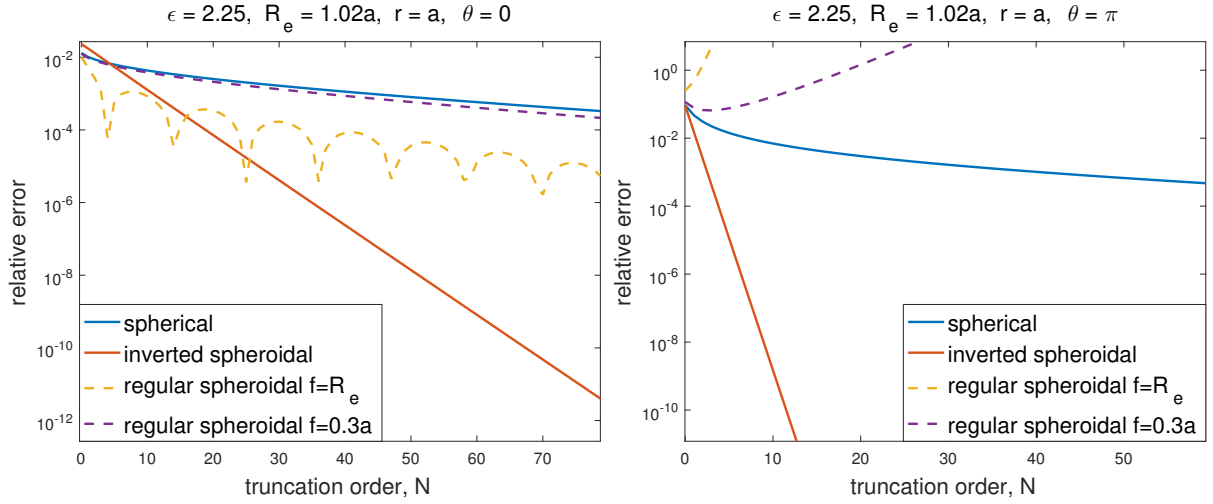


FIG. 2. Comparison of the convergence rates of the internal potential series using spherical (Eq. 3), inverted spheroidal (Eq. 13), and regular spheroidal harmonics with $f = R_e$ (Eq. 16) and $f = 0.3a$ (Eq. 17). This is quantified as the relative error between the N^{th} partial sum and the “converged” result. In this example, the point source is located at $0.02a$ from a sphere with permittivity $\epsilon = 2.25$. Note that the results are qualitatively ϵ -independent, except for extreme values such as for perfect conductors or $\epsilon = -1$. We compute the internal potential at two opposite points, $\theta = 0$ (left) and $\theta = \pi$ (right) on the sphere surface $r = a$ (where the convergence is slowest).

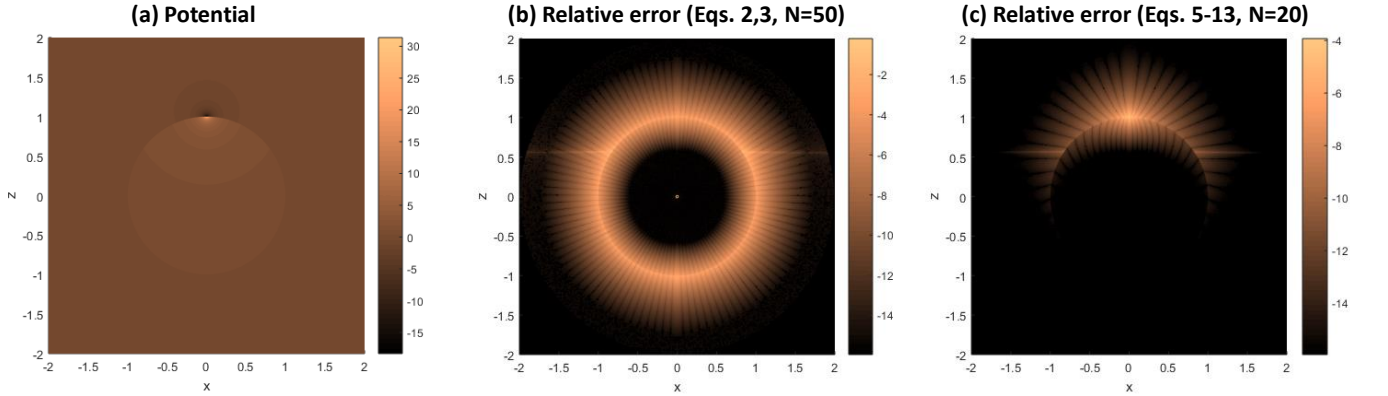


FIG. 3. Surface maps of the solution for a point charge located at $z = R_e = 1.02a$ just outside a sphere of radius $a = 1$ and relative dielectric constant $\epsilon = 2.25$. (a) Plots of the converged solutions for the inside potential \bar{V}_{in} and reflected potential \bar{V}_r , computed from Eqs. 5 and 13 with $N = 130$ terms in the series. (b-c) Corresponding plots of the relative error (in \log_{10} scale) using the spherical harmonics series with $N = 50$ (b) or the spheroidal harmonics series with $N = 20$ (c). The horizontal line around $z = 0.5$ is due to the reflected potential being very small here, which makes the relative error large. The dark radial lines in (b-c) correspond to regions where the approximate solution coincidentally crosses the exact solution because it oscillates spatially around the correct value.

and now involves irregular spherical harmonics rather than regular.

We can therefore apply the expansion of irregular solid spherical harmonics of $(\tilde{r}, \theta, \phi)$ in terms of offset irregular spheroidal harmonics (see Eq. A3), which can be written as:

$$\left(\frac{\check{R}_e}{\check{r}}\right)^{n+1} P_n(\cos \theta) = \sum_{k=n}^{\infty} (-1)^{n+k} \frac{2(2k+1)(k+n)!}{n!(k-n)!} Q_k(\check{\xi}) P_k(\check{\eta}). \quad (11)$$

The “radially-inverted offset spheroidal coordinates” $\check{\xi}, \check{\eta}$ are:

$$\check{\xi} = \frac{\check{r} + \check{r}'}{\check{R}_e} = \frac{R_e}{r} + \sqrt{\frac{R_e^2}{r^2} - \frac{2R_e \cos \theta}{r} + 1},$$

$$\check{\eta} = \frac{\check{r} - \check{r}'}{\check{R}_e} = \frac{R_e}{r} - \sqrt{\frac{R_e^2}{r^2} - \frac{2R_e \cos \theta}{r} + 1}, \quad (12)$$

$$\text{where } \check{r}' = \sqrt{\check{r}^2 - 2\check{r}R_e \cos \theta + \check{R}_e^2}.$$

Their domains are $\check{\xi} \in [1, \infty)$, $\check{\eta} \in [-1, 1]$, the same as for non-inverted spheroidal coordinates. Eq. 11 is valid

everywhere except for $\check{\xi} = 1$ or equivalently $\theta = 0$, $0 \leq \check{r} \leq R_e$, which corresponds to the infinite segment on the positive z -axis with $z > R_e$ (outside the sphere).

Following Ref. [1], we then substitute the expansion in Eq. 11 into Eq. 10, change the order of summation, re-label $k \leftrightarrow n$ and use Eq. 6 to obtain

$$\bar{V}_{\text{in}} = \frac{2\bar{V}_q}{\epsilon + 1} + 2\beta_\infty \frac{a}{r} \sum_{n=0}^{\infty} (2n+1)c_n Q_n(\check{\xi}) P_n(\check{\eta}), \quad (13)$$

which is valid everywhere inside the sphere. As was found for the external potential, the spheroidal harmonic expansion in Eq. 13 converges much faster than the standard solution as shown in Figs. 2-3.

This improved convergence is related to the singularity of the solution. An integral form of the potential was found in [5] using the method of images:

$$\bar{V}_{\text{in}} = \frac{2\bar{V}_q}{\epsilon + 1} + \frac{a}{R_e} \frac{\epsilon\beta_\infty}{\epsilon + 1} \int_{R_e}^{\infty} \frac{(R_e/\check{z})^\mu d\check{z}}{\sqrt{x^2 + y^2 + (z - \check{z})^2}}. \quad (14)$$

The last term is the the potential created by an infinite line charge on the z axis for $z \geq R_e$. This corresponds exactly to $\check{\xi} = 1$, i.e. to the singularity of $Q_k(\check{\xi})$, which makes the inverted spheroidal harmonics an ideal basis for the problem.

This method could also be applied to dipole point sources for example, following the method presented in [1].

III. PROBLEMS WITH SOLUTIONS IN TERMS OF REGULAR SPHEROIDAL HARMONICS

We now analyze why it is impractical to expand the internal potential on a basis of regular spheroidal harmonics. The regular spherical harmonics in Eq. 8 can be expanded in terms of offset regular spheroidal harmonics just as can be done for the irregular harmonics; in fact the expansion is finite:

$$\left(\frac{r}{R_e}\right)^n P_n(\cos\theta) = \sum_{k=0}^n \frac{n!(2k+1)}{(n-k)!(n+k+1)!} P_k(\check{\xi}_e) P_k(\check{\eta}_e). \quad (15)$$

Eq. 15 appears new and is proved in the Appendix. Note that the offset spheroidal coordinates $(\check{\xi}_e, \check{\eta}_e)$ are here defined with O and E as foci, not O and I as used for the reflected potential. The expansion coefficients of the internal potential in terms of regular spheroidal harmonics can be found by substituting Eq. 15 into the potential given in Eq. 8, rearranging the order of summation and relabeling $n \leftrightarrow k$:

$$\bar{V}_{\text{in}} = \frac{2\bar{V}_q}{\epsilon + 1} + \frac{a\beta_\infty}{R_e} \sum_{n=0}^{\infty} (2n+1)d_n P_n(\check{\xi}_e) P_n(\check{\eta}_e), \quad (16)$$

$$\text{where } d_n = \sum_{k=n}^{\infty} \frac{1}{k(\epsilon + 1) + 1} \frac{k!^2}{(k-n)!(k+n+1)!}.$$

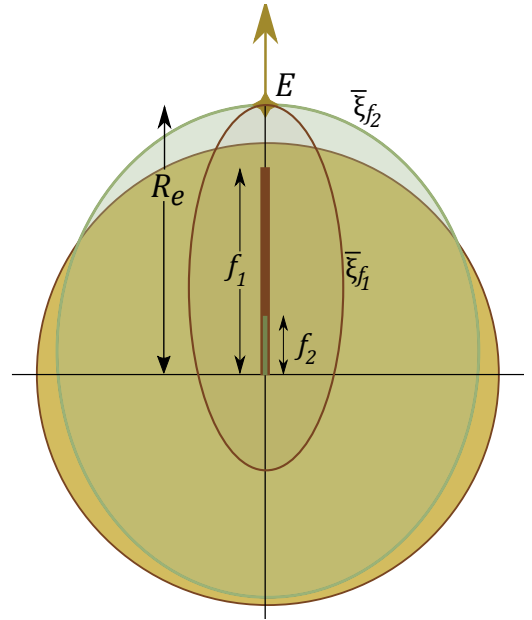


FIG. 4. Boundary of convergence for the series solution expressed on two different bases of offset regular spheroidal harmonics of focal lengths f_1 and f_2 . Any series of regular spheroidal harmonics will diverge outside some spheroid and converge (to a finite value) inside. The spheroid must be small enough so that it excludes the singularity of the analytic continuation of the series, which extends from point E $z = R_e$ for the internal potential. A choice of a larger focal length will mean that the spheroid boundary is too thin and the series will diverge for most of the interior of the sphere. If the focal length is very small, the boundary of convergence approaches a sphere, the same spherical boundary that defines the convergence of the standard spherical solution, but the spheroidal harmonics also reduce to spherical harmonics.

The sum over k in the definition of d_n converges, but we could not find a simple closed form of these coefficients as was the case for c_n in the solution of the reflected potential (Eq. 6).

The problem in Eq. 16 lies with the region of convergence of the series (of n). One can expect that the boundary of divergence will be the largest spheroid (constant $\check{\xi}_e$) which does not cross the singularity of the analytic continuation of the series (see App. C for proof). But the singularity extends from point E to infinity and any spheroid with $\check{\xi}_e > 1$ crosses this line. Consequently the series only converges for $\check{\xi}_e = 1$ – on the z axis for $0 \leq z \leq R_e$ – ideally we need it for all $r \leq a$. As illustrated in Fig. 2, while there is a small improvement in the convergence rate of this series at $r = a, \theta = 0$, the series diverges on the other side at $r = a, \theta = \pi$.

To avoid this problem, we search for a solution using offset spheroidal coordinates $(\check{\xi}_f, \check{\eta}_f)$ centered on O and F=(0, 0, f), with a smaller focal length f , as shown in Fig. 4. Writing $(r/R_e)^n = (r/f)^n (f/R_e)^n$ and using Eq. 15 substituting f for R_e , we obtain after the same ma-

nipulations:

$$\bar{V}_{\text{in}} = \frac{2\bar{V}_q}{\epsilon + 1} + \frac{a\beta_\infty}{R_e} \sum_{n=0}^{\infty} (2n+1)e_n P_n(\bar{\xi}_f) P_n(\bar{\eta}_f), \quad (17)$$

$$\text{where } e_n = \sum_{k=n}^{\infty} \frac{(f/R_e)^k}{k(\epsilon+1)+1} \frac{k!^2}{(k-n)!(k+n+1)!}.$$

The region of convergence of this series is again bounded by the spheroid surface (constant $\bar{\xi}_f$) that touches the base of the image singularity, i.e. it is defined by $\bar{\xi}_f \leq 2R_e/f - 1$. For a smaller f , this region can be larger than before where we had $f = R_e$, see Fig 4. By choosing $f \leq R_e - a$, the region of convergence even contains the entire sphere $r \leq a$, as desired. However, for a point source close to the sphere, we then have $f \ll a$, i.e. F approaches O , and the spheroidal harmonics will then approach the spherical harmonics (up to some normalization), so the series convergence becomes similar to the standard solution in spherical coordinates. Besides, this spheroidal harmonic series is impractical as the coefficients e_n are also defined as a slowly-converging infinite sum.

Finally, we note that we could have used in this discussion the regular spheroidal harmonics centered about the origin instead of the offset ones, but it does not remove the issues discussed above. Overall, all attempts at finding a solution in terms of regular spheroidal harmonics result in either series that do not converge over the entire interior sphere or in series that converge everywhere inside, but at a rate comparable with the original spherical harmonic solution.

IV. POINT CHARGE INSIDE SPHERE

The method of finding spheroidal harmonic solutions presented in Sec. II and [1] can be adapted to other problems and we here present the results for the case where the point source is located inside the dielectric sphere. Again the spherical series are slowly convergent if the point source is close to the sphere surface, and the spheroidal series converge much faster.

The problem is almost the same as in Fig. 1 but now with the source located at point I ($z = R_i$), and the image charge at E. The potential inside the sphere ($r \leq a$) is written as $\bar{V}_{\text{in}} = \bar{V}_q + \bar{V}_r$, where \bar{V}_q is the potential due to the point charge and \bar{V}_r the reflected potential. We now expand \bar{V}_q on a series of irregular solid spherical harmonics centered at the origin:

$$\bar{V}_q = \frac{a}{|\mathbf{r} - R_i \hat{\mathbf{z}}|} = \frac{a}{R_i} \sum_{n=0}^{\infty} \left(\frac{R_i}{r}\right)^{n+1} P_n(\cos \theta) \quad (r > R_i) \quad (18)$$

The standard solution for the reflected potential (inside

the sphere, $r \leq a$) is

$$\bar{V}_r = \sum_{n=0}^{\infty} \frac{(n+1)(\epsilon-1)}{n(\epsilon+1)+1} \left(\frac{r}{R_e}\right)^n P_n(\cos \theta), \quad (19)$$

where $R_e = a^2/R_i$ as before. The outside potential is ($r \geq a$):

$$\bar{V}_{\text{out}} = \frac{a}{R_i} \sum_{n=0}^{\infty} \frac{2n+1}{n(\epsilon+1)+1} \left(\frac{R_i}{r}\right)^{n+1} P_n(\cos \theta). \quad (20)$$

These expressions are very similar to the ones obtained for the point source outside the sphere (Eqs. 2 and 3) and the spheroidal harmonic solutions can therefore be obtained using the same arguments. We first separate the image charge for the reflected potential inside the sphere:

$$\bar{V}_r = \frac{\beta_\infty R_e}{|\mathbf{r} - R_e \hat{\mathbf{z}}|} + \sum_{n=0}^{\infty} \frac{\beta_\infty \epsilon}{n(\epsilon+1)+1} \left(\frac{r}{R_e}\right)^n P_n(\cos \theta). \quad (21)$$

From there, we recognize up to a factor the same series as in Eq. 8, so we use the Kelvin transformation method and obtain in terms of spheroidal harmonics:

$$\bar{V}_r = \frac{\beta_\infty R_e}{|\mathbf{r} - R_e \hat{\mathbf{z}}|} + 2\beta_\infty \epsilon \frac{R_e}{r} \sum_{n=0}^{\infty} (2n+1)c_n Q_n(\bar{\xi}) P_n(\bar{\eta}). \quad (22)$$

For the outside potential, the approach in [1] can be used directly to find:

$$\bar{V}_{\text{out}} = \frac{2\bar{V}_q}{\epsilon+1} + 2\frac{a\beta_\infty}{R_i} \sum_{n=0}^{\infty} (2n+1)c_n Q_n(\bar{\xi}) P_n(\bar{\eta}). \quad (23)$$

V. DISCUSSION AND CONCLUSION

This work demonstrates that spheroidal harmonics provide a more suitable basis for the solution of Laplace's equation for a point source near a sphere. Despite the irregular spheroidal harmonics being an ideal basis for the external potential, regular spheroidal harmonics are *not* a suitable basis for the internal potential. Instead, the Kelvin transformation can be used to find solution in terms of irregular spheroidal harmonics of a new type of coordinates: radially-inverted offset spheroidal coordinates. Essentially the problem has been transformed with a radial inversion, turning the sphere inside out, and solved the problem of finding the potential outside this transformed sphere using the method in [1]. Similar radially-inverted coordinate systems, other than the inverted offset prolate spheroidal coordinates, were also discussed by Moon and Spencer [8]. Interestingly, a similar inverted coordinate system has also been recently investigated in the context of fluid dynamics [9], although

with the spheroidal coordinates centered about the origin.

In general, if $f(r, \theta, \phi)$ satisfies Laplace's equation, then $f(r \rightarrow a^2/r, \theta, \phi)/r$ is also a solution [2]. So the functions $Q_n(\check{\xi})P_n(\check{\eta})/r$ solve Laplace's equation. Since the non-inverted irregular spheroidal harmonics are suitable for modelling potentials that go to zero at infinity, the inverted harmonics should be suitable for potentials that are finite at the origin. The corresponding isopotentials, i.e. surfaces where $Q_n(\check{\xi})P_n(\check{\eta})/r$ are constant, are shown in Appendix D.

The internal potential solution presented here reinforces the interpretations discussed in [1] and further highlights the connection with solutions in terms of the method of images [5, 6]. The solution in a given region of space has a unique analytic continuation with well-defined singularities, independently of the series expansions chosen to calculate it. The best (most rapidly convergent) basis functions for the problem are likely those with singularities that match the singularity of the solution. In the case of the external potential for an external point source at E, the singularity is a line between O and I, and spheroidal harmonics of the offset coordinates $\bar{\xi}, \bar{\eta}$ exactly match this. In the case of the internal potential for an external point source at E, the singularity is a line extending from the point source at E to infinity and the radially-inverted offset spheroidal harmonics match exactly that singularity. In fact, our expansions could have been derived from the integrals of the image theory solutions using the Havelock formula [10, 11], which for our offset spheroidal coordinate system can be re-expressed as:

$$Q_n(\bar{\xi})P_n(\bar{\eta}) = \frac{1}{2} \int_0^{R_i} \frac{P_n(2\tilde{z}/R_i - 1)}{\sqrt{x^2 + y^2 + (z - \tilde{z})^2}} d\tilde{z}. \quad (24)$$

The Legendre polynomials in the numerator are a basis

for functions defined on the interval $0 \leq \tilde{z} \leq R_i$. This makes $Q_n(\check{\xi})P_n(\check{\eta})$ a basis for any charge distribution on the segment OI, and the expansion will converge in all space (except the line segment). A similar expression can be written for the radially-inverted offset spheroidal coordinate system:

$$\frac{Q_n(\check{\xi})P_n(\check{\eta})}{r} = \frac{1}{2} \int_{R_e}^{\infty} \frac{P_n(2R_e/\tilde{z} - 1)/\tilde{z}}{\sqrt{x^2 + y^2 + (z - \tilde{z})^2}} d\tilde{z}. \quad (25)$$

so $Q_n(\check{\xi})P_n(\check{\eta})/r$ are natural functions for expressing semi-infinite line singularities. We believe these considerations could be fruitful in devising new approaches to improve the solutions of many related problems of mathematical physics.

Appendix A: Relationships between spherical and spheroidal harmonics

In [1] we presented two new expansions relating spherical and offset spheroidal harmonics in the case of offset spheroidal coordinates defined for a general $c > 0$ as:

$$\bar{\xi}_c = \frac{r + r'_c}{c}, \quad \bar{\eta}_c = \frac{r - r'_c}{c}, \quad (A1)$$

$$\text{where } r'_c = |\mathbf{r} - c\hat{\mathbf{z}}| = \sqrt{r^2 - 2cr \cos \theta + c^2}.$$

In the text, those coordinates are used with $c \equiv R_i$ to express solutions outside the sphere.

We reproduce those expansions below for completeness and refer to [1] for their proofs:

$$P_n^m(\bar{\xi}_c)P_n^m(\bar{\eta}_c) = \frac{(n+m)!}{(n-m)!} \sum_{k=m}^n \frac{(-)^{n+k}}{k!(k+m)!} \frac{(n+k)!}{(n-k)!} \left(\frac{r}{c}\right)^k P_k^m(\cos \theta), \quad (A2)$$

$$\left(\frac{c}{r}\right)^{n+1} P_n^m(\cos \theta) = \frac{2(-)^{n+m}}{n!(n-m)!} \sum_{k=n}^{\infty} (-)^k (2k+1) \frac{(k+n)!}{(k-n)!} \frac{(k-m)!}{(k+m)!} Q_k^m(\bar{\xi}_c)P_k^m(\bar{\eta}_c). \quad (A3)$$

We also present and prove the inverse expansions, of which Eqs. 15 and C3 are special cases. These are

$$\left(\frac{r}{c}\right)^n P_n^m(\cos \theta) = n!(n+m)! \sum_{k=m}^n \frac{2k+1}{(n-k)!(n+k+1)!} \frac{(k-m)!}{(k+m)!} P_k^m(\bar{\xi}_c)P_k^m(\bar{\eta}_c) \quad (A4)$$

$$Q_n^m(\bar{\xi}_c)P_n^m(\bar{\eta}_c) = \frac{(-)^m}{2} \frac{(n+m)!}{(n-m)!} \sum_{k=n}^{\infty} \frac{k!(k-m)!}{(k-n)!(k+n+1)!} \left(\frac{c}{r}\right)^{k+1} P_k^m(\cos \theta). \quad (A5)$$

Similar relationships have been given and proved in the

case of the standard spheroidal coordinates centered at

the origin [12–14]. Eq. A4 is proved in the next section. Eq. A5 can be proved following the same method used to prove Eq. A3 in [1] so the proof is not repeated here.

Appendix B: Proof of Eq. A4

Knowing that Eq. A2 holds and is a finite invertible basis transformation, it must be possible to find the inverse expansion:

$$\left(\frac{r}{c}\right)^n P_n^m(\cos \theta) = \sum_{k=m}^n \alpha_{nk}^m P_k^m(\bar{\xi}) P_k^m(\bar{\eta}). \quad (\text{B1})$$

Substitute this into Eq. A2, and rearrange the order of summation to get

$$P_n^m(\bar{\xi}) P_n^m(\bar{\eta}) = \frac{(n+m)!}{(n-m)!} \sum_{p=m}^n \sum_{k=p}^n \frac{(-)^{n+k}}{k!(k+m)!} \frac{(n+k)!}{(n-k)!} \alpha_{kp}^m P_p^m(\bar{\xi}) P_p^m(\bar{\eta}).$$

Since $P_n^m(\bar{\xi}) P_n^m(\bar{\eta})$ are orthogonal functions, we must have

$$\frac{(n+m)!}{(n-m)!} \sum_{k=p}^n \frac{(-)^{n+k}}{k!(k+m)!} \frac{(n+k)!}{(n-k)!} \alpha_{kp}^m = \delta_{np}. \quad (\text{B2})$$

The coefficients α_{kp}^m can be deduced by looking at the orthogonality relation for the shifted Legendre polynomials $P_n(2x-1)$:

$$\int_0^1 P_n(2x-1) P_p(2x-1) dx = \frac{\delta_{np}}{2p+1}. \quad (\text{B3})$$

Now expand the shifted Legendre polynomials in powers of x :

$$\begin{aligned} \frac{\delta_{np}}{2p+1} &= \int_0^1 \sum_{k=0}^n \frac{(-)^{n+k} (n+k)!}{k!^2 (n-k)!} x^k \sum_{q=0}^p \frac{(-)^{q+p} (q+p)!}{q!^2 (p-q)!} x^q dx \\ &= \sum_{k=0}^n \frac{(-)^{n+k} (n+k)!}{k!^2 (n-k)!} \sum_{q=0}^p \frac{(-)^{q+p} (q+p)!}{q!^2 (p-q)!} \frac{1}{k+q+1}. \end{aligned} \quad (\text{B4})$$

The sum over q can be simplified by using Eq. 6 with $n \rightarrow p$, $k \rightarrow q$, $\mu \rightarrow k+1$)

$$\sum_{q=0}^p \frac{(-)^{q+p} (q+p)!}{q!^2 (p-q)!} \frac{1}{k+q+1} = \frac{k!^2}{(k-p)!(k+p+1)!}. \quad (\text{B5})$$

Substituting this back into Eq. B4 we have

$$\sum_{k=0}^n \frac{(-)^{n+k} (n+k)!}{(n-k)!(k-p)!(k+p+1)!} = \frac{\delta_{np}}{2p+1}. \quad (\text{B6})$$

Compare this with Eq. B2 to find that α_{nk}^m are in fact the coefficients given in Eq. A4. \square

Appendix C: Boundary of convergence of Eq. 17

Here we prove that the boundary of convergence of Eq. 17 is a spheroid whose surface touches point E. To do this we look at the limit as $n \rightarrow \infty$ of the terms in the series. The asymptotic form of the Legendre polynomials $P_n(u)$ for $|u| < 1$ is [15] (pp 304-306):

$$P_n(u) \rightarrow \sqrt{\frac{2}{\pi n \sqrt{1-u^2}}} \sin \left(\left(n + \frac{1}{2} \right) \cos^{-1} u + \frac{\pi}{4} \right), \quad (\text{C1})$$

which applies to $P_n(\bar{\eta}_f)$. For $P_n(\bar{\xi}_f)$, we need the asymptotic form for $|u| > 1$:

$$P_n(u) \rightarrow \frac{(u + \sqrt{u^2 - 1})^{n+1/2}}{\sqrt{2\pi n} (u^2 - 1)^{1/4}}. \quad (\text{C2})$$

To determine the asymptotic form of the sum over k , we evaluate Eq. A5 (with $c \rightarrow f$) at $\cos \theta = \eta_f = 1$:

$$\sum_{k=n}^{\infty} \frac{k!^2}{(k-n)!(k+n+1)!} \left(\frac{f}{r} \right)^{k+1} = 2Q_n(\bar{\xi}_f). \quad (\text{C3})$$

Integrating this expression with respect to $v = \bar{\xi}_f = 2r/f - 1$ from $r = \infty$ to $r = R_e$:

$$\sum_{k=n}^{\infty} \frac{k!^2 (f/R_e)^k}{(k-n)!(k+n+1)!} \frac{-1}{k} = \int_{\infty}^{2R_e/f-1} Q_n(v) dv. \quad (\text{C4})$$

As $n \rightarrow \infty$, the left hand side is proportional to the sum over k in Eq. 17. Evaluating the right hand side:

$$\int_{\infty}^u Q_n(v) dv = \frac{uQ_n(u) - Q_{n+1}(u)}{n+1}. \quad (\text{C5})$$

The asymptotic form of $Q_n(u)$ for $|u| > 1$ is [15]

$$Q_n(u) \rightarrow \frac{\sqrt{\pi/2/n}}{(u^2 - 1)^{1/4} (u + \sqrt{u^2 - 1})^{n+1/2}}, \quad (\text{C6})$$

so that

$$\int_{\infty}^u Q_n(v) dv \rightarrow \frac{\text{constant}}{n^{3/2} (u + \sqrt{u^2 - 1})^n}. \quad (\text{C7})$$

Putting all this together, the n^{th} term in the series in Eq. 16 approaches

$$\frac{\text{constant}}{n} \left(\frac{\bar{\xi}_f + \sqrt{\bar{\xi}_f^2 - 1}}{2R_e/f - 1 + \sqrt{(2R_e/f - 1)^2 - 1}} \right)^n P_n(\bar{\eta}). \quad (\text{C8})$$

Let X be the expression in the large brackets. If $X < 1$ (equivalent to $\bar{\xi}_f < 2r/f - 1$) it is clear that the series converges since it is bounded by the series $\sum X^n/n$ which converges. For $X > 1$ ($\bar{\xi}_f > 2R_e/f - 1$), the series diverges because the terms increase in size. Geometrically, the boundary of convergence is the surface of a spheroid with foci at $z = 0$ and $z = f$ that passes through point E at $R_e \hat{z}$.

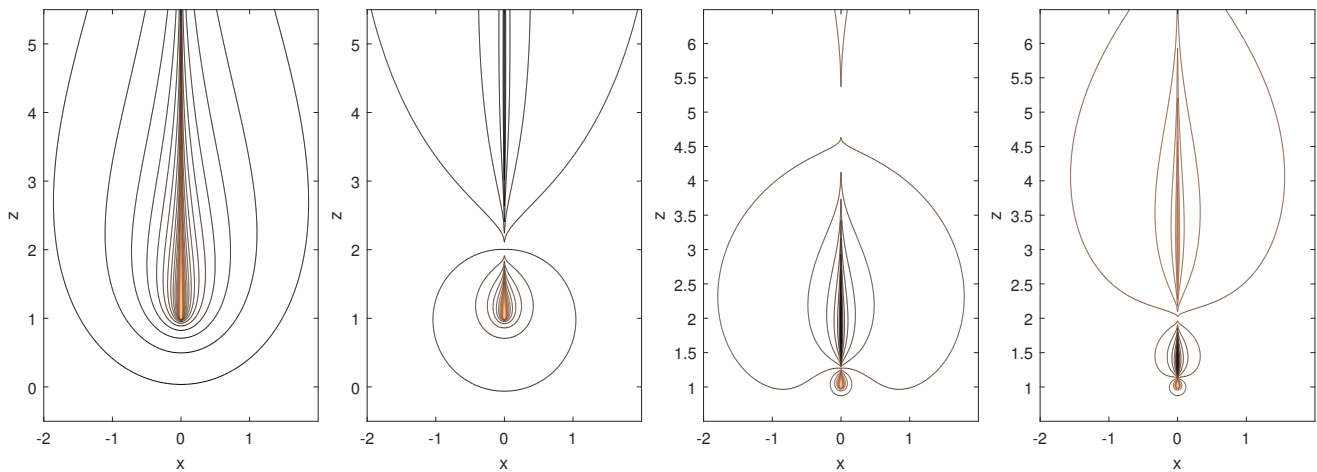


FIG. 5. Isopotentials of the functions $Q_n(\check{\xi})P_n(\check{\eta})/r$ for $n = 0, 1, 2, 3$ from left to right. The focal length of the non-inverted spheroidal coordinates is 1, so that they are singular on the z -axis from $z = 1$ to ∞ .

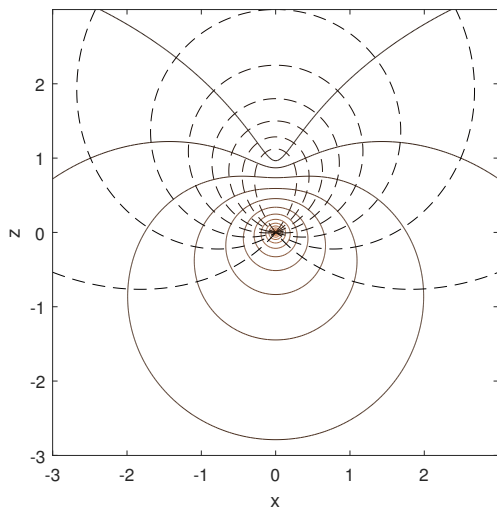


FIG. 6. Constant coordinate surfaces on the plane $y = 0$. Surfaces of constant $\check{\eta}$ (dashed lines) range from a finite line on the z -axis for $\check{\eta} = 1$ to sharply dimpled spheres for $\check{\eta} < 0$. $\check{\xi}$ range from small spheres for large $\check{\xi}$ to smoothly dimpled spheres as $\check{\xi} \rightarrow 1$. The focal length of the coordinates is 1.

Appendix D: Inverted spheroidal coordinates surfaces

Here we further illustrate the properties of the inverted spheroidal coordinates $(\check{\xi}, \check{\eta})$. We graph the isopotentials of the first few orders of the harmonics $Q_n(\check{\xi})P_n(\check{\eta})/r$ in Fig. 5. We also plot the surfaces of constant $\check{\xi}$ and $\check{\eta}$ in Fig. 6.

ACKNOWLEDGEMENTS

This work was supported by the MacDiarmid Institute of advanced materials and nanotechnology, and a Victoria doctoral scholarship.

-
- [1] M. R. A. Majić, B. Auguie, and E. C. Le Ru, *Phys. Rev. E* **95**, 033307 (2017).
 - [2] W. Thomson, *Journal de Mathématiques Pures et Appliquées* **12**, 256 (1847).
 - [3] G. Dassios, *IMA J. Appl. Math.* **74**, 427 (2009).
 - [4] R. Amaral, O. Ventura, and N. Lemos, *European Journal of Physics* **38**, 025206 (2017).
 - [5] I. V. Lindell, *Radio Science* **27**, 1 (1992).
 - [6] J. C.-E. Sten and I. V. Lindell, *Microwave and optical technology letters* **5**, 597 (1992).
 - [7] J. A. Stratton, *Electromagnetic theory* (McGraw-Hill, New York, 1941).
 - [8] D. E. S. a. Parry Moon, *Field Theory Handbook: Including Coordinate Systems, Differential Equations and Their Solutions* (Springer Berlin Heidelberg, 1961).
 - [9] M. Hadjinicolaou and E. Protopapas, *IMA J. Appl. Math.* **80**, 1475 (2015).
 - [10] T. H. HAVELOCK, *Quart. J. Mech. Appl. Math.* **5**, 129 (1952).
 - [11] T. Miloh, *SIAM J. Appl. Math.* **26**, 334 (1974).
 - [12] G. B. Jeffery, *Proceedings of the London Mathematical Society* **s2-16**, 133 (1917).
 - [13] G. Jansen, *J. Phys. A: Math. and General* **33**, 1375 (2000).
 - [14] V. A. Antonov and A. S. Baranov, *Technical Physics* **47**, 80 (2002).
 - [15] E. W. Hobson, *The theory of spherical and ellipsoidal harmonics* (CUP Archive, 1931).